KERNFORSCHUNGSZENTRUM

KARLSRUHE

Juni 1967

KFK 607

Institut für Experimentelle Kernphysik

A Novel Time-of-Flight Method and its Applications in Nuclear Reaction Studies

H. Brückmann, E.L. Haase, W. Kluge, L. Schänzler

GESELLSCHAFT FÜR KERNFORSCHUNG M. B. H.

KARLSRUHE

GESELLSCHAFT FÜR KERNFORSCHUNG M. B. H.
KARLSRUHE

KERNFORSCHUNGSZENTRUM KARLSRUHE

Juni 1967 KFK 607

Institut für Experimentelle Kernphysik

A Novel Time-of-Flight Method and its Applications in Nuclear Reaction Studies [+)]

H. Brückmann, E.L. Haase, W. Kluge and L. Schänzler

Gesellschaft für Kernforschung m.b.H., Karlsruhe

+) submitted to Nucl. Instr. & Meth.

Abstract

A time-of-flight method designed for accelerators with high particle burst rates is described. The method uses an independent energy measurement to resolve the ambiguity which arises when the primary pulse separation, length of flight path and energy range are outside the limits of conventional time-of-flight technique.

The system can be used for an accurate determination of the energy of neutrons and charged reaction products, for very precise calibration of the primary beam energy and for particle identification in case of charged reaction products.

The method is being used at the Karlsruhe isochronous cyclotron for nuclear reaction studies. In the course of our investigations of the cyclotron beam properties, we measured burst widths down to 0.2 nanoseconds.

The methods discussed below extend the application of time-of-flight technique to situations where a high repetition rate of the primary beam burst prohibits the use of the conventional time-of flight technique (see for example [1, 2]). There the permissible repetition rate of the beam bursts is limited by the length of the flight path and the energy range of the particles to be detected. This limit is due to the necessity of avoiding that particles from different beam bursts are able to overtake each other on their flight path. Methods which remove these limits were developed at the Karlsruhe isochronous cyclotron and are in use since 1964. These techniques will be discussed with reference to this cyclotron, but they are generally applicable to all particle accelerators with high beam pulse repetition rates.

The Karlsruhe isochronous cyclotron [+)], a fixed-energy machine, is able to accelerate protons, deuterons or α-particles to an energy of 25 MeV/nucleon. From its special design properties it was expected that this cyclotron would be able to produce extremely short beam bursts. This special feature arises primarily from the unconventional application of a 3-Dee RF system with six acceleration gaps [3,4].

The central region of this accelerator is shown in the schematic drawing of fig. 1. The three dees are mechanically and electrically coupled in the cyclotron center and fed with RF at this center point. Consequently, the ion source had to be mounted off center. The first orbit is geometrically well defined by a set of slits mounted in the dees.

The very short beam bursts one is able to achieve with this special geometry are primarily caused by two properties:

Firstly, the RF frequency is three times higher than for a conventional one-dee cyclotron. The system is fed with 33 MHz (which corresponds to a 30 nsec length of period). Secondly, and mainly due to the defining properties of the inner slits, a small phase acceptance angle can be achieved by proper adjustment of the ion

+) designed and built by AEG, Frankfurt

source and RF amplitude. This first orbit phase angle is further decreased in the course of the acceleration. As a consequence, beam pulses of 0.2 to 0.5 nsec length can be achieved with a fixed repetition rate of 33 MHz.

These facts indicate that for investigations of nuclear reactions a suitable time-of-flight technique could be used advantageously. Ordinarily, the fact that the time between two pulses is as short as 30 nsec would imply a severe upper limit on the length of flight paths, that could be used. This is because particles from successive pulses must be prevented from overtaking each other on their flight paths.

The resolution of a time-of-flight measurement is inversely proportional to the length of the flight path. This clearly contradicts the requirement to avoid overtaking at repetition rates as high as 33 MHz. Two methods employed at our cyclotron try to overcome this general difficulty:

1. A method for producing intense pulsed neutron beams was developed by Cierjacks and Beckurts [5,6,7]. In this method two out of three successive beam pulses are eliminated near the center of the cyclotron. Additionally, a pair of deflecting plates brings about 50 beam bursts from neighbouring orbits simultaneously into an internal target. This method is able to produce neutron bursts of 1 nsec width with repetition rates of 20 kHz and is in current use for precise measurements of neutron cross sections.

2. Our method was developed for investigations of nuclear reactions with the external beam [8,9,10,11]. This method is based on the idea of using all beam pulses but resolving the ambiguity due to particles which might overtake each other on their flight paths. It is based on a precise time difference measurement and an independent rough energy determination. The principle of operation

will be described in detail in part I of this paper. Part II contains a description of the electronic system, and in part III a few examples for application in nuclear reaction studies will be mentioned.

I: Time-of-flight method

Non-relativistically, the time of flight τ can be written

$$\tau = \sqrt{\frac{m}{2E}} \cdot l \qquad (1)$$

(m mass, E kinetic energy of the particle, l length of flight path)

From this equation one can evaluate the range of times of flight to be expected for the problem under investigation.

In our case we are interested in studying the reaction products n, p, d, He^3, and α-particles in the energy range between 10 and 100 MeV and we want to be able to use flight paths between 0.5 and 8 m. By inserting these numbers into equation (1) one finds that the range of the expected times of flight extends roughly from 10 to 200 nsec. With the beam pulse separation of 30 nsec the above mentioned basic requirement for time-of-flight technique cannot be realized offhand. Particles created by different beam pulses are able to overtake each other. This is illustrated in fig. 2. Here we assume for simplicity that only neutrons are detected. This figure shows in the upper part the neutron energy versus time of flight. In the lower part the arrival time of the successive beam pulses S_1, S_2, ... is shown. The point marked 'T', for instance, represents the arrival time of a neutron at the detector and $\Delta\tau$ should be the corresponding time difference referred to the preceding beam pulse. It is obvious that neutrons with energies E_1,

E_2, E_3 from the beam pulses S_1, S_2, and S_3 are able to arrive simultaneously at the detector. The chain of the pulses S_i has a periodic structure and only the time difference $\Delta\tau$ to the preceding beam pulse is significant for timing an event. The total time of flight has to be evaluated from

$$\tau = \Delta\tau + n \cdot \tau_o \qquad (2)$$

and the integer n = 1, 2 , ... has to be extracted from a second independent measurement. As can be seen from fig. 2 a rough energy measurement is sufficient for this purpose. The required energy resolution has to be good enough only to allow a distinction between the different branches in field 3. After determination of n, formula (2) is used for the determination of the total time of flight. The exact energy of the particle is then given by the relativistic expression for formula (1). Experimentally, the position of the reference pulses S_1 can be calibrated by using the prompt γ-radiation from the target.

For determination of the neutron energy in the range between 10 and 60 MeV a proton recoil telescope had to be designed. Since only medium energy resolution is required, we were able to make its efficiency much higher than that achieved with conventional recoil telescopes [1].

The telescope used consists of two flat scintillators. The first scintillator of 0,5 - 2 cm thickness 'radiates' the recoil protons. Part of the proton recoil energy is lost already in this scintillator. The rest of the recoil energy is lost in a second scintillator of the same size which is placed 20 to 40 cm behind the first one. The size and distance of the two scintillators determine the range of the recoil angles which are accepted. This geometry is adjustable

to the specific problem under investigation. The two scintillator output pulses are added electronically. This sum is a measure of the total proton recoil energy and determines the neutron energy with an accuracy which is limited by the geometry. The timing signal for the determination of the time of flight is taken directly from the first scintillator output.

A fast coincidence circuit is needed to register only those events where both scintillators give rise to an output pulse higher than the threshold. For the experimental data shown in fig. 3 the telescope was used with a first scintillator of 1 cm thickness and a second scintillator 2 cm thick. The efficiency is high compared with a conventional recoil telescope with a thin radiator foil, and we are able to achieve values of a few times 10^{-4} for 50 MeV neutrons [8,9,10,11].

As an example, experimental data for neutrons from the $^{12}C(d,n)$ reaction are shown in fig. 3. A thin ^{12}C target was bombarded with 52 MeV deuterons. The neutrons were detected at an angle of $\vartheta_{Lab} = 20^{o}$ with the proton recoil telescope. The flight path was 8.40 meters. A map display with an array of 128 x 32 channels is shown on a two-dimensional multichannel analyser. The recoil energy of the protons E_p is displayed versus the previously defined time $\Delta\tau$. These data correspond to the area marked 'field 3' in fig. 2. It can be recognized that the different branches are well resolved. The vertical bands are caused mainly by those events where the recoil proton does not lose all its energy in the two scintillators. The one-dimensional neutron spectrum is obtained by summing over the width of the ridge along the branches. In this example the main features of the resulting spectrum are these: The peak at the highest neutron energy is due to the $^{12}C(d,n)^{13}N$ reaction to the ground state of ^{13}N; the second one is due to the unresolved first three exited levels in ^{13}N; the continuum at lower energies comes from the deuteron break-up reaction.

Formula (2) directly shows one advantage of this method. The time τ_o is fixed by the RF frequency of the cyclotron and this can be determined easily with an accuracy of 10^{-5} to 10^{-6}. This means that the second term in the expression (2), which in many cases is much larger than the first term, contributes very little to the error in the total time of flight. Hence, the relative accuracy of τ turns out to be much better than the accuracy which can be achieved with the $\Delta\tau$ measurement alone.

So far the method was discussed only for neutrons. Of course it is equally applicable to charged reaction products. The three important applications are these:

a) Energy determination of reaction products

If long flight paths are used, a very accurate and absolute energy determination can be made. Conventionally, magnetic analysers or solid state detectors are used for this purpose. The absolute calibration procedure of these systems is a labourious task, compared with the time-of-flight system where only a length and a time have to be calibrated in absolute units.

b) Calibration of primary beam energy

A second application of the time-of-flight method is the energy calibration of an accelerator beam. The use of this method yields absolute and very precise values for the energy; in addition information on energy spread and beam properties can be obtained. This will be discussed in detail in part III for the Karlsruhe isochronous cyclotron.

c) Particle Identification

A third application for charged particles offers a very simple way of particle identification. In our case flight paths down to 40 cm can be used. Fig. 4 shows an example of the detection of

protons, deuterons and tritons from reactions induced in boron by 51.5 MeV deuterons. This result differs from fig. 3 only by the fact that due to the different masses each kind of particle has its own distinct set of branches. It is evident from this map display, that the different masses are separated very well. A similar particle identification using the time-of-flight technique has been applied independently at other laboratories [12, 13, 14, 15].

If one compares the commonly used $\frac{dE}{dx}$ - E particle identification technique with the time-of-flight method one finds that such a time measurement contains additional information. In principle, the signals from a $\frac{dE}{dx}$ - E telescope contain only information on those properties of the particles which are specific at the time when the particles cross the telescope. By comparison, the time-of-flight method contains also information on the previous history of the detected particle. The curves t = f(E) of fig. 2 are valid only for particles, which travel along the flight path with a constant energy. If they lose energy by slit scattering between the target and detector, or if they cause a reaction in the detector, or even if they are created in between by another unwanted reaction, these events will not be registered on the curve t=f(E).

Such additional information can be obtained also for that part of the whole process where the primary beam particle travels from the accelerator to the target. As can be seen from the discussion of the principle of operation, no essential difference arises when a constant time interval is added to $\Delta\tau$. If one chooses as time reference the departure time from the cyclotron, the interval corresponds to the time of flight between the cyclotron and the target. Then the resulting information will contain also the primary energy and the energy distribution of the primary beam. To include this option and for convenience we are using a reference timing signal deduced from the RF of the cyclotron.

II: Electronic system

For the application of the method discussed in part I a suitable electronic system was designed. There are four main experimental aspects which will govern the overall performance of the entire system. They will be discussed in the following sections.

a) The length of the primary beam pulse determines the accuracy within which the 'starting time' of a reaction product from the target is known. The accelerator should be operated so that the shortest possible beam pulse is obtained.

To investigate the properties of the primary beam measurements were made by bombarding a thick Cu target with a well focused external beam. Prompt γ-rays and neutrons were detected with a scintillation counter placed at a distance of 30 cm from the target. Fig. 5 shows a typical result for such a burst width measurement. The number of counts is plotted versus the time difference $\Delta\tau$. The time scale is 51 psec/channel. A narrow peak arising from the γ-rays is seen on the left side and the neutron spectrum gives rise to the broad distribution on the right side. Since a measurement like this includes the time jitter of the detector and the effects of the finite size of the beam spot and the scintillation crystal, it must be concluded that in this example the beam pulse had a halfwidth of less than 0.25 nsec. Under optimum conditions and for short operation periods widths of less than 0.2 nsec have been achieved. Over long periods we have operated the cyclotron with a pulse width of 0.3 - 0.4 nsec.

b) The determination of the 'arrival time' of a particle has to be carried out in such a way that the detector contributes a minimum of time jitter. Moreover the energy of the particle should not influence the position of the timing signal from the detector. This second attribute is particulary important in cases where neutrons are detected via their recoil protons.

To meet these requirements a special tunnel diode circuit was designed for the use with photomultipliers. The circuit is based on a zero crossing method and contains also the character of a discriminator. Since such a design is of interest in many different fields of nuclear research work, the circuit and its specific characteristics will be discussed in a separate paper [16]. Listed below are only some typical results for the performance achieved. The timing of a 50 MeV deuteron is possible with an uncertainty of $\pm$ 30 psec. This number contains all effects arising from the crystal phototube assembly and from the whole electronic system used. The time drift of the output signal can be made less than 30 psec for a variation of input amplitudes in the range of 1 : 8.

c) The determination of the time difference $\Delta\tau$ implies that, firstly, for each event the preceding beam pulse is selected out of the continuous chain of RF-pulses. Secondly, this time difference has to be converted into an amplitude. As one can see from fig. 2, there are positions for 'T' where particular care has to be taken to avoid improper behaviour of the electronics. These effects might occur when 'T' is very close to a beam pulse S_i. In such cases the measured quantity $\Delta\tau$ might either be near the maximum value of 30 nsec or be near zero. There a very small change in the position of 'T' relative to the reference pulses has to switch the output signal for $\Delta\tau$ from the maximum value to zero. Furthermore, one wishes to be completely certain that in this critical region events cannot be lost by electronic effects. Otherwise, the branches could not be fitted together without objection. Finally, an optimum for the differential linearity of the time-to-amplitude conversion is required.

If only a conventional time-to-pulse-height converter is used to measure $\Delta\tau$, the single pulse 'T' has to start the converter and the 33 MHz pulse chain 'RF' has to stop the converter. However, it

is well known that this mode of operation results in a serious nonlinearity, especially at the end points of the range. To avoid all these difficulties from the beginning we use a more elaborate but consequent way for the selection of one proper pulse out of the whole 'RF' pulse chain.

The principle of operation is shown in fig. 6. The detector pulse 'T' triggers gate generator 1 which produces a standard gate pulse of 45 nsec length. By using this pulse for gate I, a section 45 nsec long is cut out of the periodic chain of 'RF' pulses. It is important to notice that this will bring at least one and not more than two 'RF' pulses to the gate generator 2. One should notice also that some of the 'RF' pulses will be deteriorated: This occurs when the 'RF' pulse coincides with the leading edge of the gate pulse. In this case the gate I starts to open just at the time when an 'RF' pulse arrives at the input. The consequence is that such 'RF' pulses are decreased in amplitude and are shifted in time. Accordingly the output pulses from gate I cannot be used for reference purpose, but they are used to trigger another gate generator of approximately 15 nsec length. This unit triggers at about half the amplitude of the 'RF' pulses, and one has to keep in mind that if the first 'RF' pulse is degenerated so far as to be unable to trigger generator 2, there is always a second pulse which will trigger gate generator 2 properly. The 15 nsec standard pulse is able to gate a non-deteriorated reference pulse out of the delayed 'RF' pulse chain because at this point the gating signal and the gated 'RF' pulse are correlated in time. The delay time is adjusted so that the 'RF' pulse is situated in the center of the 15 nsec gating pulse. Any timing jitter will now shift this pulse only around the center of the 15 nsec gate signal and the resulting single 'RF' pulses are thus neither degenerated in amplitude nor shifted in time. Furthermore, the timing and the dead time of generator 2 are such that each pulse 'T' will generate always one and only one 'RF' pulse at the output of this circuit. After a delay the time difference $\Delta\tau$

is obtained in a conventional time-to-pulse height converter (0 - 65 nsec). Since only a 30 nsec range out of these 65 nsec is used, the converter can be operated in its region of optimum linearity.

The overall performance of this part of the electronic system can best be seen from a test where a radioactive source is used to generate the timing signals 'T'. In this case the 'T' pulses are not correlated to the 'RF' pulses and a uniform distribution over the range of 30 nsec is expected. Fig. 7 shows the result. The overall differential linearity of the whole electronic system turns out to be $\pm$ 1.5 %. The uncertainty within which the circuit decides whether 'T' is before or behind a signal 'S' is smaller than $\pm$ 100 psec. This is determined from the slopes of the spectrum.

d) Finally, it should be recalled that in addition to the timing signal one needs an energy signal. In the majority of cases a charged particle detector can be operated in such a way as to yield the timing and the energy signal simultaneously. We used organic and NaI scintillation counters as well as solid state detectors and obtained very satisfactory results. In case of neutrons an energy signal is not readily available. For this purpose we used the proton recoil telescope discussed in part I.

III: Applications

The electronic system discussed above is used for a large variety of problems in the field of nuclear reaction studies. Only three applications, which are of general interest from the viewpoint of instrumentation, will be discussed in the following. These three topics are:

a) Determination of absolute energy and energy spread of a 50 MeV deuteron beam.

b) Identification system independently showing the charge and mass of the reaction products.

c) A simple method to linearize the curves E versus $\Delta\tau$. This permits more efficient utilization of the multichannel analyser.

a) Absolute energy determinations are usually carried out with a magnetic analyser. This requires very accurate calibration of the magnetic field and the geometry. A very simple way which might even yield more accurate results is the use of the time-of-flight technique. Here only two absolute quantities, the distance L and the time of flight, have to be determined. From these quantities the velocity of the particles in the beam can be calculated directly. Our set up for the experimental investigation is shown schematically in fig. 8. At three different positions (A_1, A_2, A_3 with the distances L_{12}, L_{23}, L_{13}) copper targets can be moved into the beam tube. One detector equipped with long cables can be positioned at a distance of 30 cm from each target. This detector registers the prompt γ-radiation from the target. A second detector can be used at one of the positions for monitoring purposes, to check that the beam does not change any of its relevant properties while the first detector is moved.

The following information can be obtained from such an experiment:

First, the beam energy is determined from the relative positions of the γ-peaks with respect to time. The measured time difference between two γ-peaks is equivalent to the quantity $\Delta\tau$ defined in formula (2). This expression is used to calculate the total time of flight. The integer n can be evaluated from approximate knowledge of the beam energy or the use of two different distances L_{12} and L_{23}. The time τ_o is obtained from a frequency measurement of the cyclotron RF. The distances L_{12} and L_{23} are calibrated with a theodolite.

The typical accuracy achieved for the measurement of the time-difference $\Delta\tau$ was $\pm$ 10 psec, and this corresponds to an error of 1.5×10^{-4} in τ if a flight path of 10 m is used for 50 MeV deuterons. If the measurement of the length of the flight path introduces only a negligible error, the absolute energy of the beam is thus determined with an uncertainty of $\pm 3 \times 10^{-4}$ or $\pm$ 15 keV for 50 MeV deuterons.

Secondly, the same experiment provides information on the energy-distribution as well as time-distribution of the primary beam. This information is obtained from the shape of the γ-peaks at the three different positions. After the shape is known at the first position A_1 only an energy spread in the beam can cause a change in shape for the other positions A_2 and A_3. In the simplest case one may assume that the energy of an individual deuteron in the beam is not correlated to its position in the beam pulk. In second order allowance should be made for time-energy correlations which may result in bunching or debunching effects.

Runs were made by placing the movable detector sequentially at the positions A_1, A_2 and A_3. The result for such a run is shown in fig. 8 with a time scale of 31 psec/channel. For convenience the position of the three peaks was shifted by precisely calibrated amounts of time so that their centers coincide. As can be seen from this figure, the full width at half maximum is between 210 and 245 psec, but does not increase linearly with the distance from position A_1. Different runs showed deviations of $\pm$ 20 psec in the half widths of the peaks . The reason for this behaviour is that the cyclotron could not be operated in a completely stable manner over the time required for this experiment. So far we are only able to quote an upper limit for the mean energy spread ΔE observed in this experiment. The value is $\Delta E = \pm$ 40 keV and no conclusive evidence for bunching was observed. The measured total energy was E_d = (51.470 $\pm$ 0.015) MeV.

Since, in practice, the beam energy depends on the operating conditions of the cyclotron it is desirable to have a permanent beam energy monitor. To avoid errors which arise from instabilities of the cyclotron one also would like to register the γ-radiation from two targets simultaneously. For this purpose the system is being modified in such a way that the first target at position A_1 will stop only a fraction of the beam. A second target at position A_2 will absorb approximately the same percentage of the beam and with the aid of a routing system the measurement of the γ-radiation from detectors at both positions will be carried out simultaneously.

b) A modified identification system for charged reaction products will be discussed next. The comparison of reactions like (d,t) and (d,^{3}He) is of particular physical interest. Such investigations yield information on differences between neutron and proton transfer mechanisms.

The differences in the two cross sections are expected to be small and for a very sensitive comparison tritons and ^{3}He particles have to be registered simultaneously. If one would use a $\frac{dE}{dx}$ - E telescope, the triton peak is always near the region where deuterons are registered and the He^3 is in the neighbourhood of the α-particles. Backgrounds from intense deuteron or α-spectra will then limit the accuracy within which the comparison between the triton and ^{3}He cross sections can be made.

The time-of-flight method is only able to discriminate between different masses of the reaction products. Hence, we combined a $\frac{dE}{dx}$ - E measurement with the time-of-flight measurement to determine charge and mass of a particle separately. A thin silicon transmission detector is used to provide the timing signal as well as a dE/dx signal simultaneously. The dE/dx signal is used to generate a routing signal for particles with charge two. The total energy is obtained from the

sum of the signals from the transmission counter and a solid state detector or a NaI crystal placed directly behind the transmission counter. A typical example of the application of this method is shown in fig. 9. This figure represents a 64 x 64 channel map display of particle energy versus time of flight. On the left side particles with charge one are displayed, on the right side those with charge two. Both charge spectra were measured simultaneously.

In the example of fig. 9 a gas target filled with He^4 was bombarded with 50 MeV deuterons. In this particular case the reaction $^4He(d,t)^3He$ is of special interest. The differential cross section for this reaction should only be symmetrical about 90^o, if the pick-up probability for a neutron is identical to that for a proton and if no electrical charge polarization occurs. From an experimental point of view the reaction is unique since it allows determination of the asymmetry about 90^o by simultaneous measurement of the tritons and the ^3He particles at a given angle in the laboratory system. This example demonstrates how the mass identification of the time-of-flight method and the $\frac{dE}{dx}$ - E telescope technique can be combined to achieve a reliable comparison of (d,t) and (d,He^3) reactions.

c) The last application to be discussed is a simple linearisation of the curves E versus $\Delta\tau$. For this purpose we electronically added an adjustable fraction c of the energy signal to the $\Delta\tau$ signal. A typical example is shown in fig. 10. Here E is displayed versus $(\Delta\tau+c\cdot E)$. In this particular example ^{12}C was bombarded with 50 MeV deuterons and we were only interested in the high energy parts of the proton, deuteron and triton spectra. A thin organic transmission scintillator was used for timing and the energy of the reaction products was measured with a NaI scintillation crystal. In this case the energy signal E does not contain the energy loss in the transmission counter. As can be seen, the linearisation is quite satisfactory in view of the simplicity of the electronics used. In a more elaborate system for a single NaI counter one might use a nonlinear function of E for the addition of the E and $\Delta\tau$ signals. With a nonlinear diode network we were able to achieve an almost perfect linearisation over an energy range of 5 : 1 [17].

The discussion of the application of the time-of-flight technique described in this paper is far from being complete. As one can imagine, a variety of combinations and modifications might be applied with advantage to special physical problems of interest. In concluding we might mention only briefly the classes of nuclear reaction studies we are now carrying out at the Karlsruhe isochronous cyclotron and which utilize the method discussed above. Besides its use for differential cross section measurements [10, 11], coincidence experiments are presently carried out for the study of three-particle reactions in the region of very light nuclei [17, 18]. Another field of investigation are polarization phenomena where the method is employed for the determination of neutron polarization with Mott-Schwinger scattering [19, 20] and for asymmetry measurements in reactions using a polarized ^{3}He-target. In experiments for the investigation of the level structure of very light nuclei like ^{4}He the system is used in conjunction with solid state detectors [21].

We would like to thank Prof. H. Schopper for his continuous aid and encouragement in all stages of this work and the members of the cyclotron staff for their experienced operation of the cyclotron.

References

1 J.H. Neiler, W.M. Good in Fast Neutron Physics, Part I, 509, Eds. J.B. Marion, J.L. Fowler, New York 1960

2 Neutron Time-of-Flight Methods, Ed. J. Spaepen, Brussels 1961

A.S. Rupaal, Nucl. Instr. & Meth. 49, 145 (1967)

C.J. Oliver, B. Collinge, G. Kaye, Nucl. Instr. & Meth. 50, 109 (1967)

D. Seelinger, H. Pose, Kernenergie 10, 366 (1967)

W.Schweimer, Nucl. Instr.& Meth. 32, 190 (1967)

3 Steimel, International conference on sector-focused cyclotrons and meson factories, CERN-Bericht 63-19, 1963

4 M. Reiser, Nucl. Instr. & Meth. 13, 55 (1961)
G. Schatz, IEEE Transactions on nuclear science NS-13, No.4, 441 (1966)

5 S. Cierjacks, K.H. Beckurts, International Conf. on the study of nuclear structures with neutrons, Antwerp 1965, report No. 157

6 S. Cierjacks, B. Duelli, L. Kropp, M. Lösel, H. Schweickert, H. Unseld, IEEE Transactions on nuclear science NS-13, No. 4, 353 (1966)

7 S. Cierjacks, P. Forti, L. Kropp, H. Unseld, Proc. of AEC-ENEA Seminar on Intense Neutron Sources Santa Fe 1966

8 H. Brückmann, E.L. Haase, International conference on the study of nuclear structure with neutrons, Antwerp 1965, report No. 112

9 H. Schopper, European Conference on AVF-cyclotrons, Eindhoven 1965, Report Gesellschaft für Kernforschung Karlsruhe, KFK 410, (1965)

10 H. Schopper, IEEE Transactions on nuclear science NS-13, No. 4, 318, (1966)

11 H. Brückmann, Habilitationsschrift, Technische Hochschule Karlsruhe 1966

12 D.S. Gemell, IEEE Transactions on Nucl. Science Vol. NS-11, No. 3, 409 (1964)

13 C.W. Williams, W.E. Kiker, H.W. Schmitt, Rev. Sci. Instr. 35, 1116, (1964)

14 P.E. Cavanagh, C.F. Coleman, G.A. Gard, B.W. Ridley, J.F. Turner, Nucl. Phys. 50, 49, (1964)

15 E. Blignaut, W.R. McMurray, A. Bottega, Nucl. Instr. & Meth. 51, 102, (1967)

16 H. Brückmann, E.L. Haase, W. Kluge, L. Schänzler (to be published)

17 W. Kluge, Ph.D. Thesis, external report, Gesellschaft für Kernforschung Karlsruhe 3/67 - 4

18 H. Brückmann. W. Kluge, L. Schänzler, Phys. Lett. 24 B, 649 (1967); Z.Phys. (to be published) and Proc. Symposium on light nuclei, few body problems and nuclear forces (Brela 1967), Eds. Paic, Slaus, Gordon and Breach 1968

19 L. Schänzler, Ph.D. Thesis, Karlsruhe 1968

20 H. Brückmann, W. Kluge, L. Schänzler, Z.Phys. (to be published)

21 E.L. Haase, H. Brückmann, W. Kluge, L. Schänzler, Proc. Symposium on light nuclei, few body problems and nuclear forces (Brela 1967), Eds. Paic, Šlaus, Gordon and Breach 1968 and KFK-report 679 (1967), Gesellschaft für Kernforschung Karlsruhe

Captions of figures

Fig. 1:

Central region of the Karlsruhe isochronous cyclotron. Schematically shown are the three dees I, II and III, the ion source and the beam defining slits L, B I, B II and B III.

Fig. 2:

Schematic representation of the principle of operation. An event which is registered at the particular time T corresponds to a particle energy E_1 or E_2 or E_3. The time-energy correlation is ambigious.

Fig. 3:

Map display of the recoil proton energy E_p versus the time difference $\Delta\tau$. The neutrons were created by reactions induced by 51.5 MeV deuterons in ^{12}C. The flight path was 8.40 m and the reaction angle was 20^{o}.

Fig. 4:

Map display of the energy E versus the time difference $\Delta\tau$. Protons, deuterons and tritons from reactions induced by 51.5 MeV deuterons in boron are shown. The length of the flight path was 1.26 m. The detector was a NaI scintillation counter with a thin window.

Fig. 5:

Measurement of the length of the cyclotron beam bursts. Prompt γ-rays and neutrons were detected at a distance of 30 cm from the target.

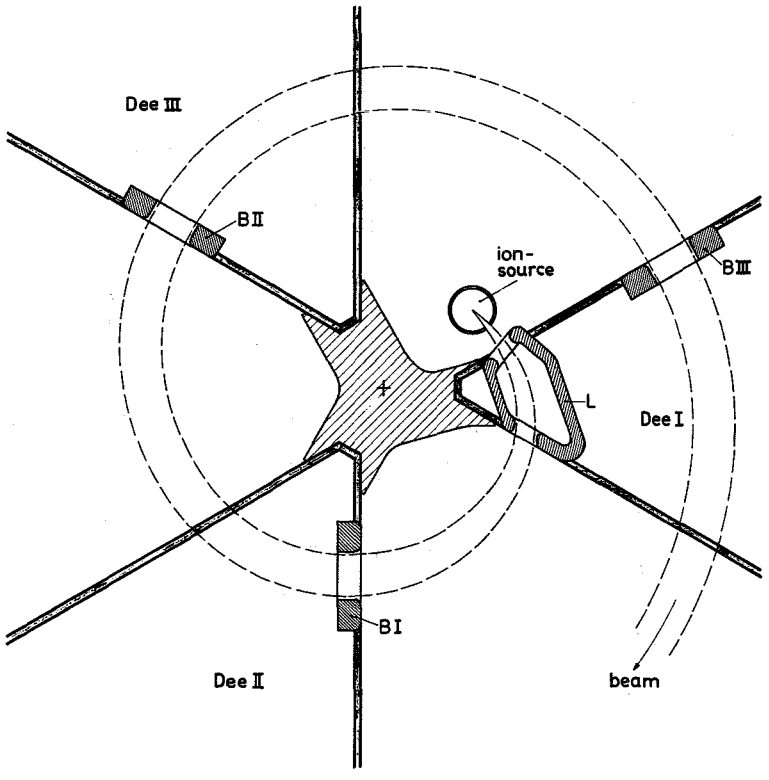

Fig. 1

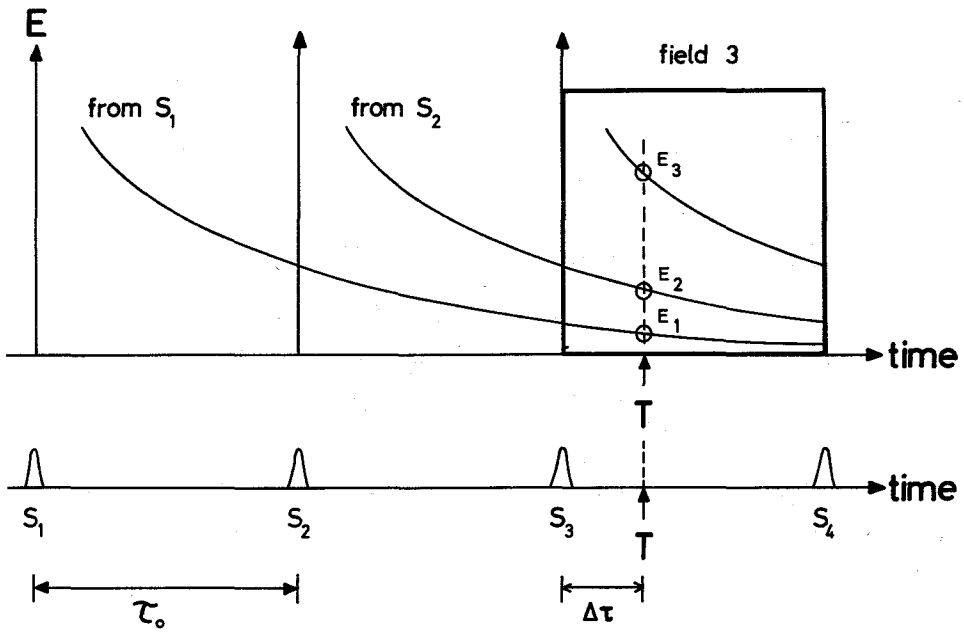
E
from S_1
from S_2
field 3
E_3
E_2
E_1
time
T
time
S_1
S_2
S_3
S_4
T
τ_o
$\Delta\tau$

Fig. 2

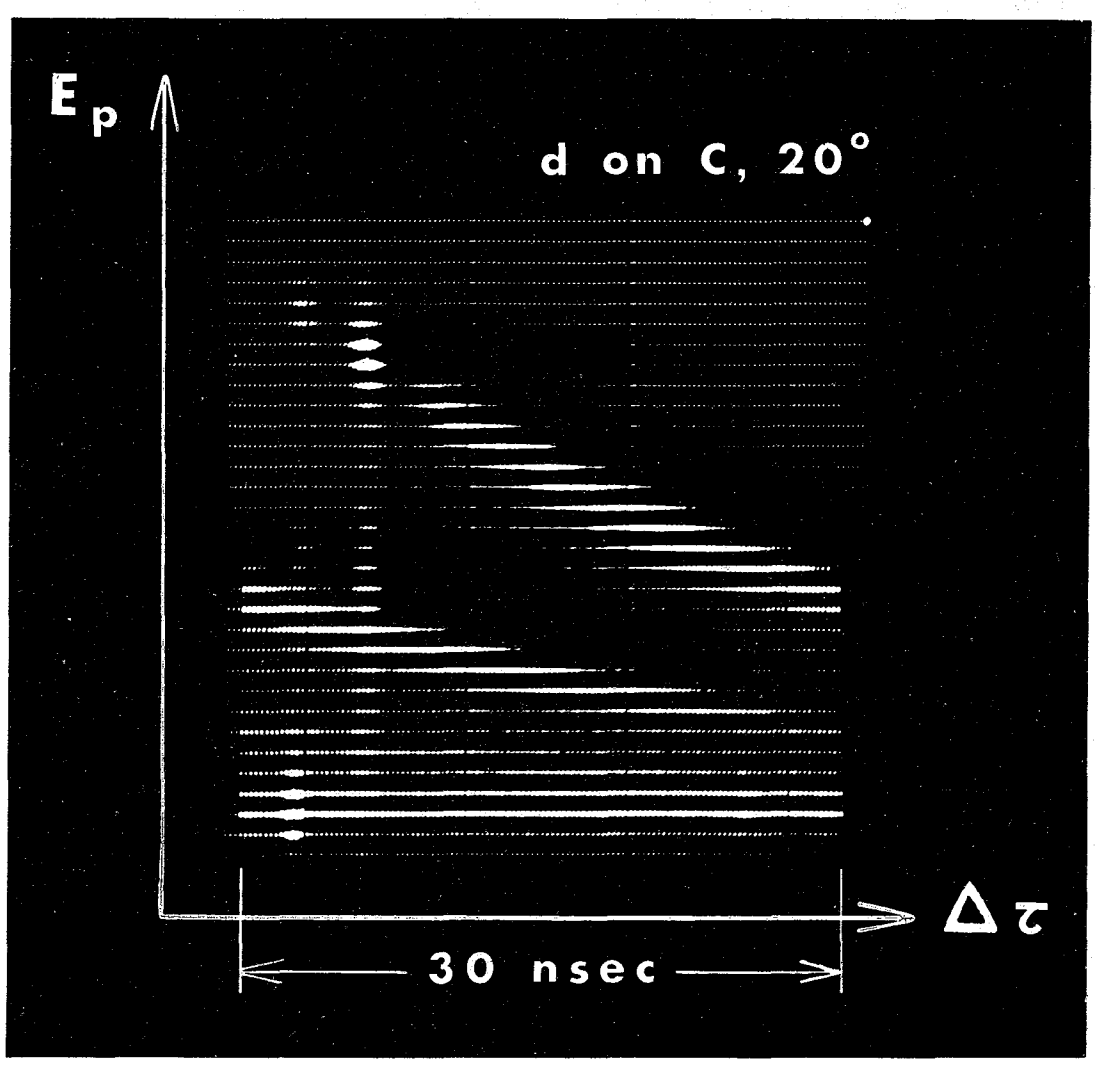

Fig. 3

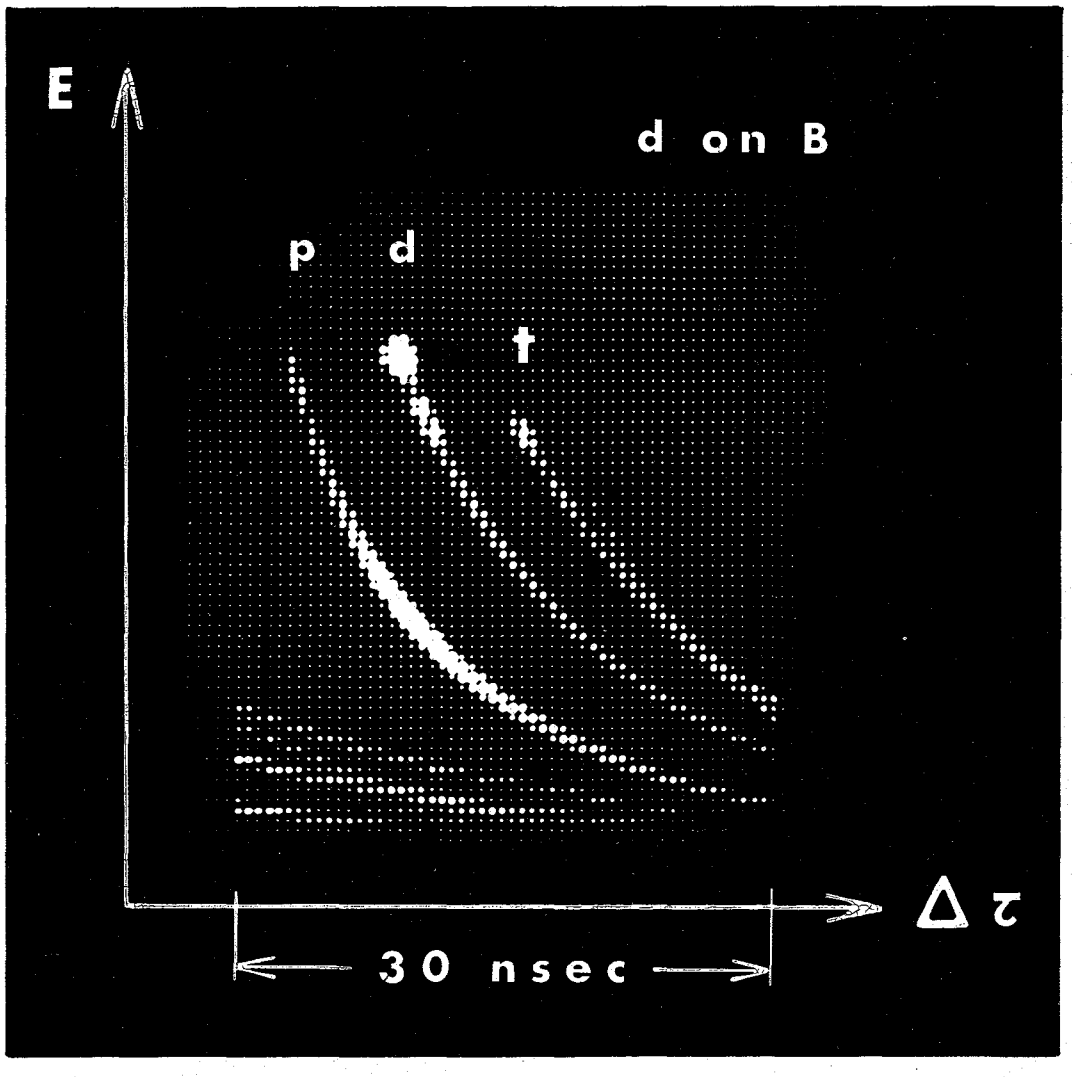

Fig. 4

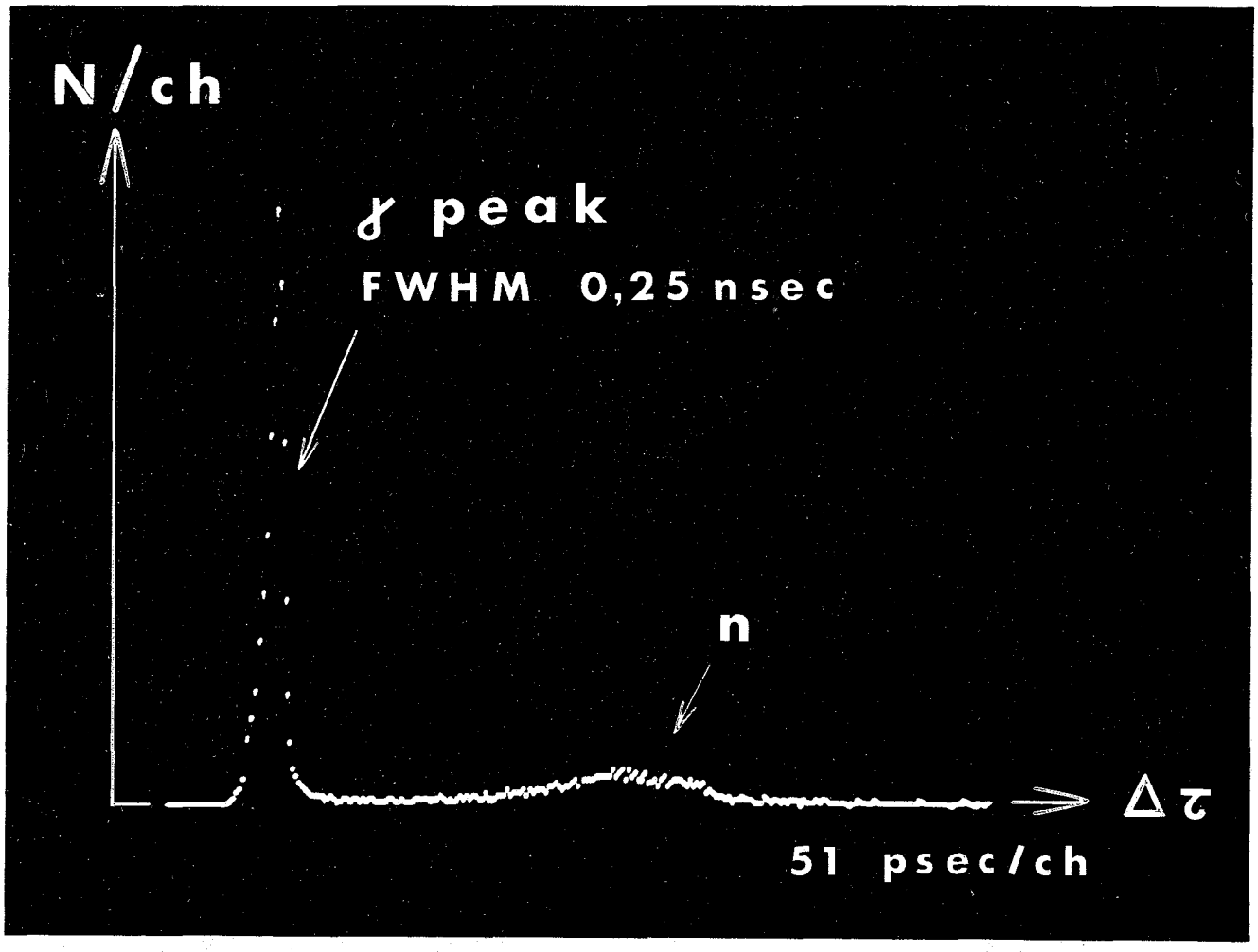

Fig. 5

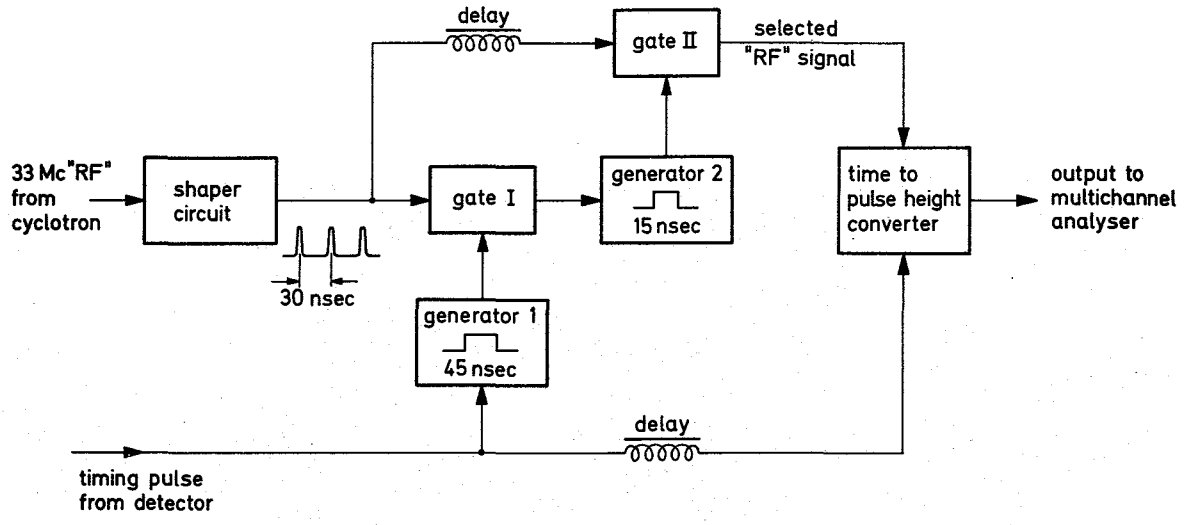
delay
gate II
selected
"RF" signal
33 Mc "RF"
from
cyclotron
shaper
circuit
gate I
generator 2
15 nsec
time to
pulse height
converter
output to
multichannel
analyser
30 nsec
generator 1
45 nsec
delay
timing pulse
from detector

Fig. 6

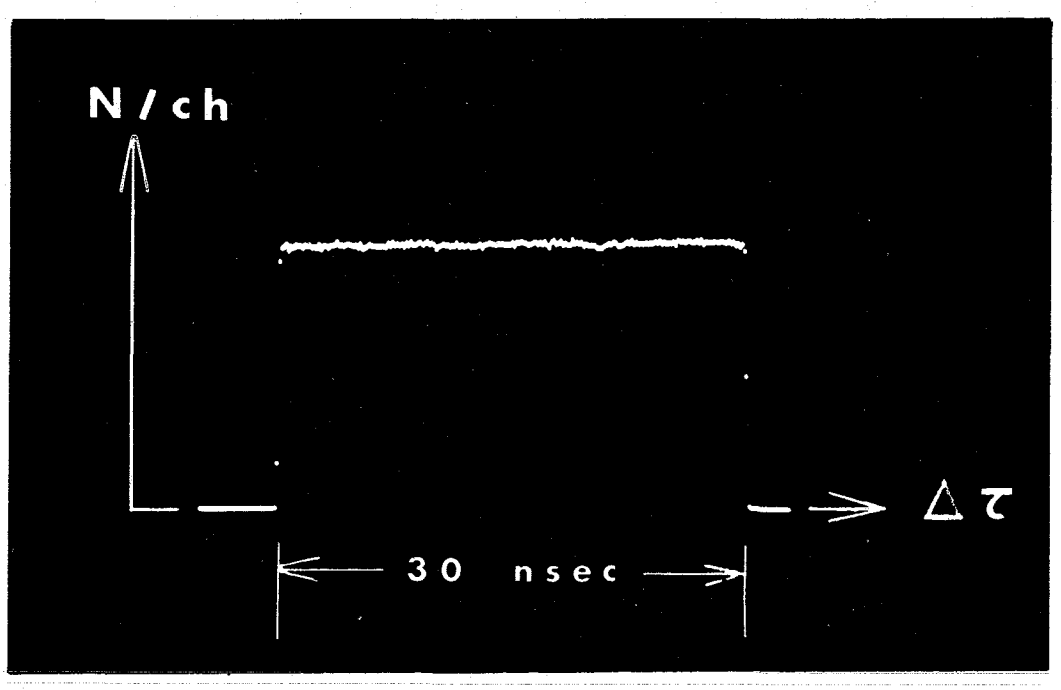
N / ch
Δ τ
30 nsec

Fig. 7

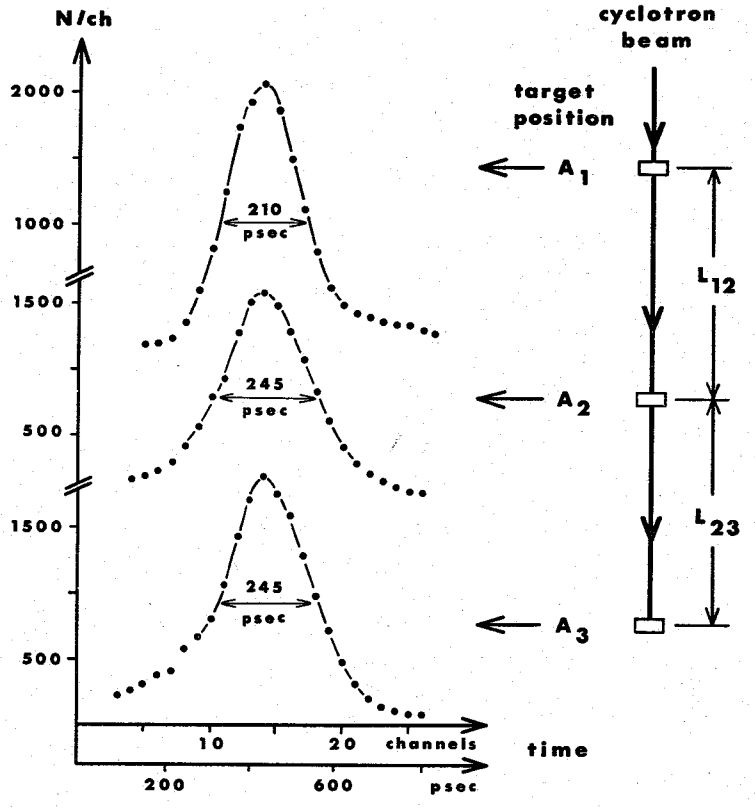
N/ch
2000
1000
1500
500
1500
500
210
psec
245
psec
245
psec
10
20
channels
200
600
psec
time
cyclotron
beam
target
position
A1
A2
A3
L12
L23

Fig. 8

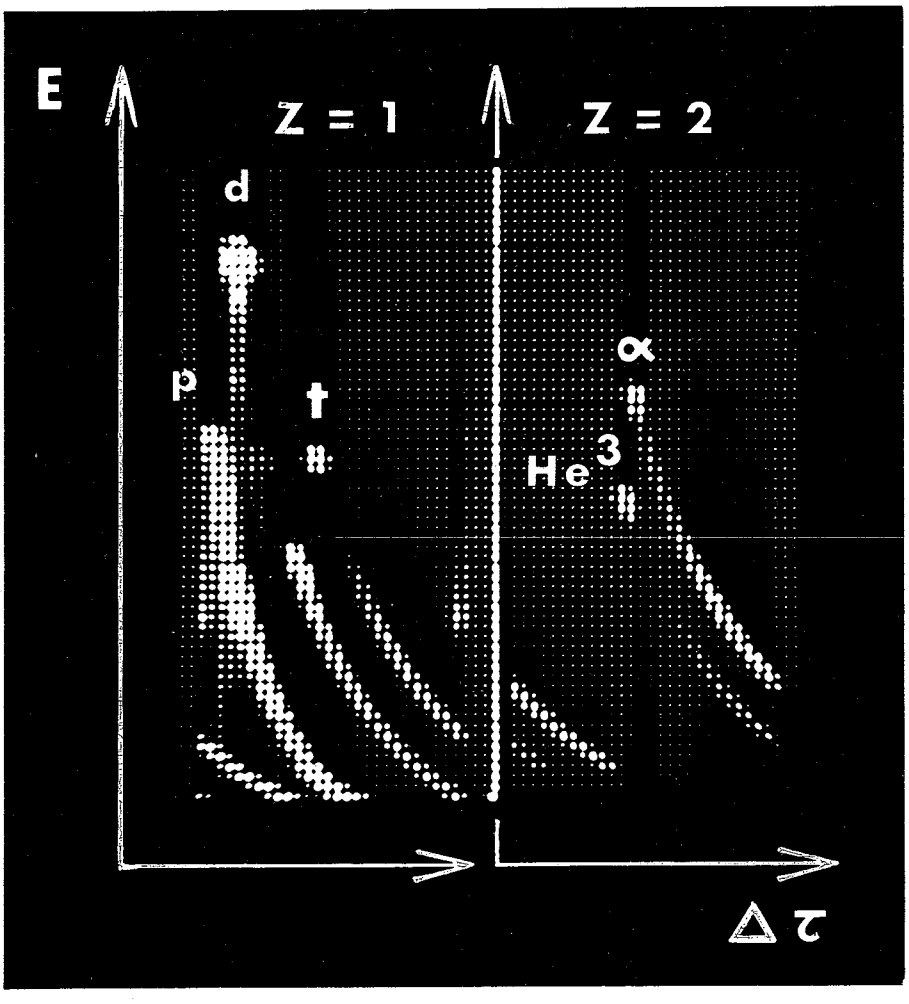

Fig. 9

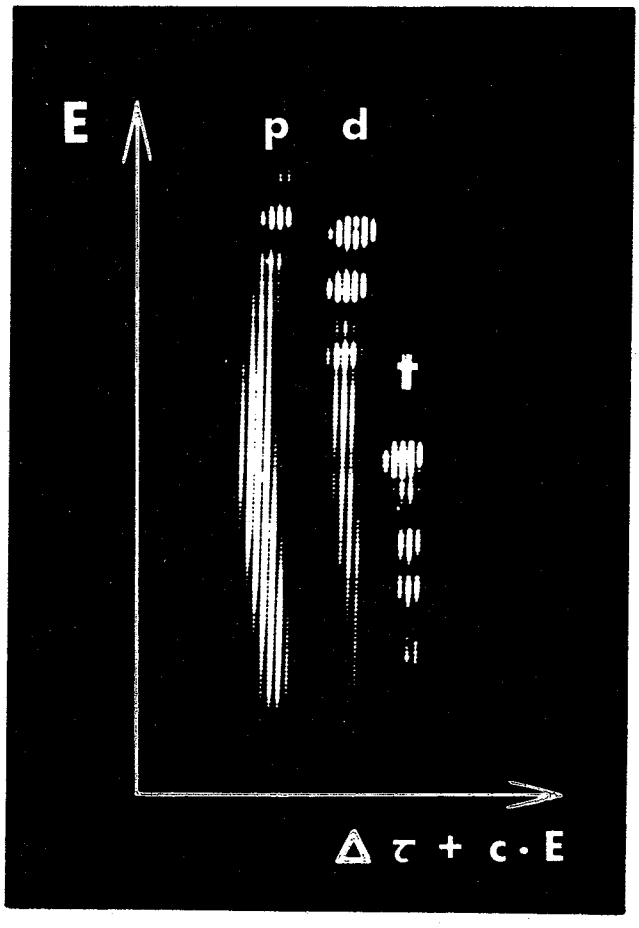

Fig. 10